Design of Near-Field Beam-Splitting Frequency Selective Surfaces for Fabry-Perot Cavity Antenna Systems

Chanjoon Lee, Robert Sainati, and Rhonda Franklin
Department of Electrical Engineering
University of Minnesota
Minneapolis, MN, USA
leex6406@umn.edu, saina002@umn.edu, rfrank01@umn.edu

***Abstract*—The effect of frequency selective surface (FSS) augmentation on the radiation of a slot or patch antenna is investigated. A variety of FSS designs comprised of horizontal and vertical slots are analyzed and compared for two sources - slot or patch. Simulations and measurements are shown for select combinations that offer near-field beam-splitting capability.**

Keywords— Fabry-Perot Cavities (FPC); frequency selective surface (FSS); antenna arrays; antenna radiation patterns

I. Introduction

Recently, near-field communication technology has become more popular because of rapid dissemination of wireless devices such as smartphones and tablets. Fabry-Perot Cavity (FPC) antenna systems have been used in a variety of areas in that beam-focusing is simply achieved with a combination of a single source and frequency selective surface (FSS) [1-5]. The FPC antenna system can also provide the potential to be used for applications such as near-field communication, imaging and sensing in short-range distance.

This paper studies how a source and frequency selective surface of the Fabry-Perot Cavity (FPC) antenna system affect beam-splitting in the near-field region and beam-recombining in the far-field region. A slot or patch antenna is combined with different FSS architectures. The simulation and measurement results are presented for various combinations of source and FSS designs. These results are analyzed to study the effect on near-field behavior, transmission response, and far-field radiation pattern performance.

II. Design

Fig. 1 shows the Fabry-Perot Cavity (FPC) antenna system. Two source antennas and three FSS designs are considered. For the source, slot and microstrip patch antenna are designed at 12GHz. The design can be described by the three main parameters: (a) the FSS design, (b) the cavity height separating the source and FSS, and (c) the source. The slot antenna is fed by a coplanar waveguide (CPW) and patch

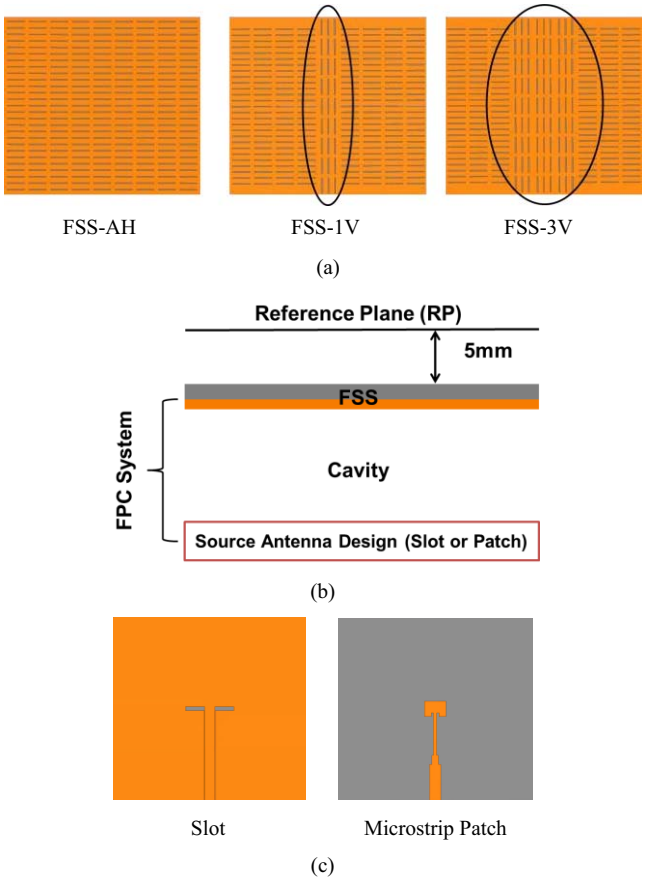

Fig. 1. FPC antenna system with three FSS arrays and two source antennas: (a) top view of the FSS designs (b) cross-section of the FPC system (c) top view of the slot (left) and patch (right) source antennas

antenna is fed by a microstrip line. The slot has a length of 22.8mm and width of 1.88mm. The patch has a length of 7.65mm and width of 9.88mm. A 50Ω CPW feedline has a signal width of 4.83mm and gap of 0.2mm. The microstrip feedline system consists of a 100Ω (length = 21.09mm), 70.7Ω (length = 4.54mm) and 50Ω (length = 17.81mm) line

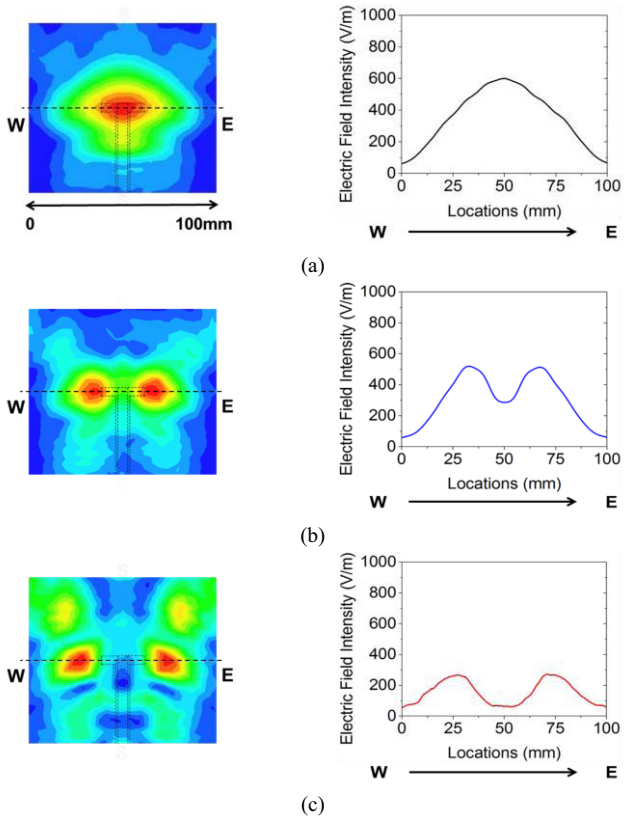

Fig. 2. Near-field distribution for FPC system with slot antenna at 11.2 GHz above each FSS (left) and electric field intensity along W-E line (right) (a) FSS-AH (b) FSS-1V (c) FSS-3V

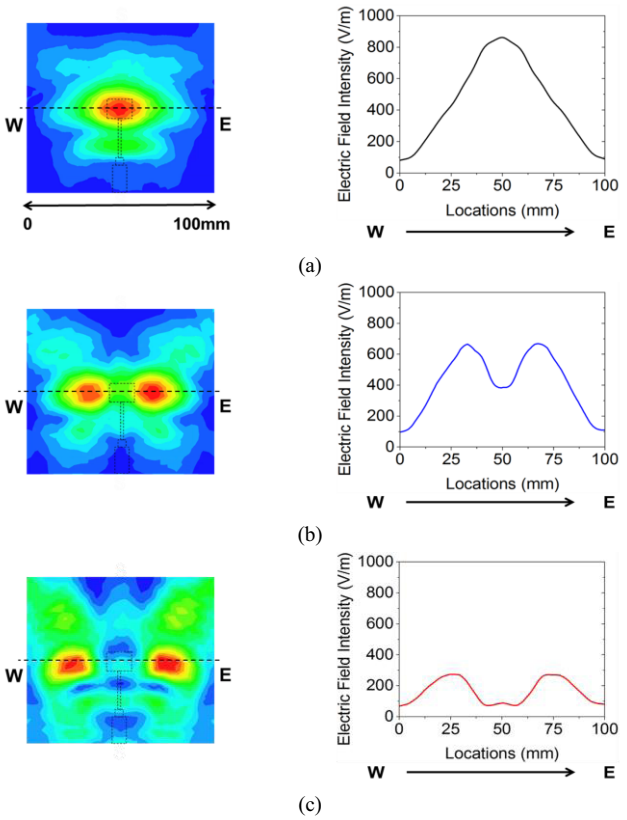

Fig. 3. Near-field distribution for FPC system with patch antenna at 11.2 GHz above each FSS (left) and electric field intensity along W-E line (right) (a) FSS-AH (b) FSS-1V (c) FSS-3V

between the patch and input port, respectively. The FSS designs, based on [6-7], have a unit cell width of 10mm and length of 3mm. A rectangular aperture is 8mm by 0.5mm and centered in the middle of the unit cell. Each FSS design has 9 columns comprised of horizontally or vertically oriented unit cells. The horizontal columns have 27 horizontally oriented unit cell rows and the vertical columns have 9 by 3 vertically oriented unit cells. Note that three vertically oriented unit cells define the width of one vertical column.

There are three FSS designs investigated. The first FSS design is the reference and is referred to as all horizontal slots (FSS-AH). The next two are combinations of horizontally and vertically oriented slots. The second FSS design has 1 vertical column centered between 4 horizontal columns and is called FSS-1V. The third design has 3 vertical columns centered between 3 horizontal columns and is referred to as FSS-3V. The height of cavity is 10.81mm.

All antenna, feedline and FSS designs are printed on Rogers Duroid5880 ($\varepsilon_r = 2.2$, substrate height = 1.57mm, metal thickness = 35μm). The FSS metal side points down in all cases. The slot antenna metal layer also points downward, but the patch antenna metal layer points upward.

III. Results

Data from ANSYS HFSS is used to model the near- and far-field behavior at a given frequency. For near-field performance, the reference plane (RP) is located 5mm above each FSS. For far-field radiation pattern, the radiation boundary encloses the reference plane (RP) as well as FPC antenna system. A port is designed as coaxial model to excite the source and illuminate the FSS structure. All simulation results presented are obtained at 11.2GHz to match the best theoretical radiation pattern of each FPC design.

A. Near-Field Distribution

The near-field behavior of FPC antenna system with slot or patch for each FSS is shown in Fig. 2 and 3, respectively. For FSS-AH design, the patch shown in Fig. 3(a) has the strongest field intensity (930V/m) and most tapered distribution compared to the slot (620V/m) shown in Fig. 2(a). The higher field intensity with the patch is due to the unidirectional radiation of the patch compared to the bidirectional radiation of the slot into the cavity of the FPC system and the air region below the FPC system.

When the vertical columns are inserted above the source and feedline, several things occur. First, the vertical columns reduce the leakage of the radiated energy from the source and line through the FSS. Second, this vertical region acts as a reflector in the cavity which reflects a stronger source signal in the horizontal column FSS regions. The resulting effect is that the main beam located over the slot or patch is split approximately equally in the 'W-E' direction. For the FSS-1V design, the two beams for slot and patch, shown in Fig. 2(b) and 3(b), have the peak intensity of 510V/m and 630V/m,

respectively. Their respective center locations are 16mm and 17mm from the center of the source antenna for the slot and patch, respectively. The minimum intensity between the two split beams is 300V/m for the slot case and 404V/m for the patch.

When the vertical column width is increased to three and the horizontal columns width is reduced to three on each side, the split beam separation increases and the orientation is no longer symmetric along a linear line. Instead it propagates along an arc angle with respect to the antenna center. Moreover, additional beams arise in the plane along the off-axis angle. Widening the reflected vertical surface in FSS-3V, as shown in Fig. 2(c) and 3(c), results in a lower beam level because the extra vertical slots prevent the source energy from leaking through the FSS. It also causes energy redistribution in the horizontal slot region that creates two beams on each side with different intensities. Both the slot and patch have similar near-field distribution.

B. S-parameter Response

The measurement results are obtained using the Anritsu 37369D Network Analyzer. A full two-port calibration is used to establish the reference planes at the SMA connector interface to the board.

To evaluate the beam-splitting capability, a microstrip open stub sensor is designed and fabricated on Duroid5880 ($\varepsilon_r = 2.2$, substrate height = 0.508mm, metal thickness = 17.5μm). Fig. 4 illustrates the test circuit with the sensor. The microstrip has a width of 1.57mm and length of 45mm. Each stub is separated by a center to center spacing of 25mm. For measurements, port 1 from the network analyzer (NA) is connected to a source antenna located at P1 of the FPC system as input. The other ports of the sensor are terminated with 50Ω load while port 2 from the NA is connected to the n^{th} port of the sensor as the output. Copper tape is used to connect the SMA connector to the FSS that behaves as a slotted ground plane. The sensor at 5mm above each FSS is assembled with the FPC antenna system to replicate the HFSS model. The range of the line impedance is 208 ~ 243Ω.

The measured S-parameter response is shown in Fig. 5. The solid line (P3) represents the sensor line located in the center of the slot or patch. The lines (P2 and P4) with symbols are

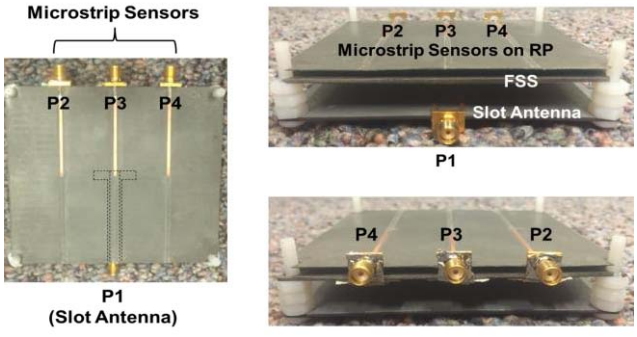

(a) (b)

Fig. 4. Picture of the test circuit with the microstrip sensors (a) top view (b) cross-section view

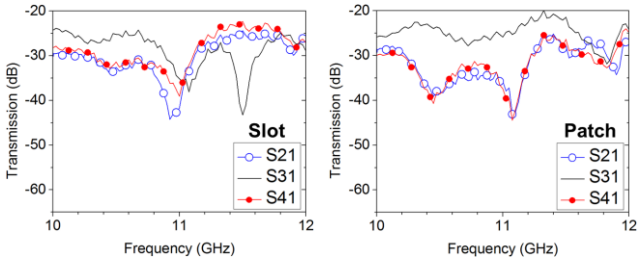

(a) FSS-AH

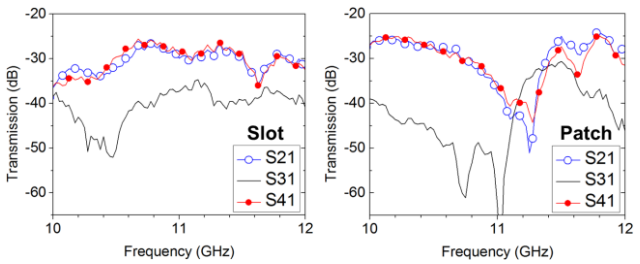

(b) FSS-3V

Fig. 5. Measured S-parameters (dB) vs. frequency (GHz): FPC system with slot (left) or patch (right)

located above the horizontal column region of the FSS approximately 25 mm from the center. In all cases, P2 (S21) and P4 (S41) responses are expected to produce similar results due to FPC symmetry. The radiation pattern discussed in section C, shows the best pattern occurring at 10.81GHz and 10.85GHz for the slot and patch respectively, in the FSS-AH case. Therefore, in Fig. 5(a), it can be shown that the signal (S31) over the antenna in both cases has a higher field intensity compared to the field strength locations at P2 (S21) and P4 (S41). The patch, however, has the largest field strength difference, which is consistent with the narrow field distribution for the patch compared to the distribution for the slot shown in Fig. 2(a). In Fig. 5(a), the patch signal level for at P2 (S21) and at P3 (S31) is -35dB and -25dB whereas for the slot signal strength is -30dB and -25dB, respectively. For FSS-3V design, the beam is also split, therefore, P3 signal is much lower than the P2 and P4 and over a broader range of frequencies compared to the FSS-AH design. The optimum beam-splitting occurs for the slot (20dB) at 10.5GHz and for the patch (40dB) at 11GHz in Fig. 5(b).

C. Far-Field Radiation Pattern

The simulated radiation pattern is shown in Fig. 6. The FSS-AH, FSS-1V and FSS-3V will be presented in this section. The E-plane pattern is along the direction of the feedline and the antenna. The H-plane pattern is horizontal across the center of the antenna. Each figure compares the response of the different FSS designs with each source antenna.

The E-plane pattern is shown in Fig. 6(a). The asymmetry in the E-plane pattern is due to the feedline location in the plane of the antenna. For the FSS-AH design, the peak gain for slot is 14.6dBi and for patch is 15.82dBi. The beamwidth for slot is 24˚ and for patch is 27˚. The slot has more back lobe because of the bidirectional radiation of the slot. For FSS-1V, the peak gain for slot is 12.84dBi and for patch is 14.71dBi.

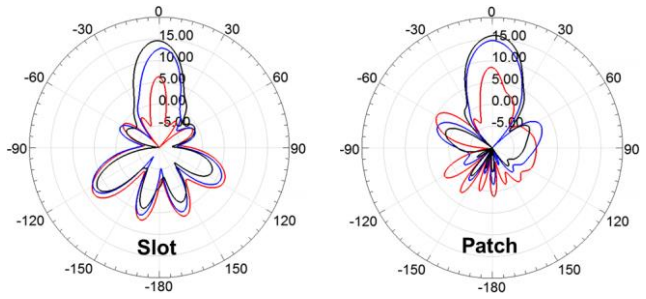

(a) E-plane

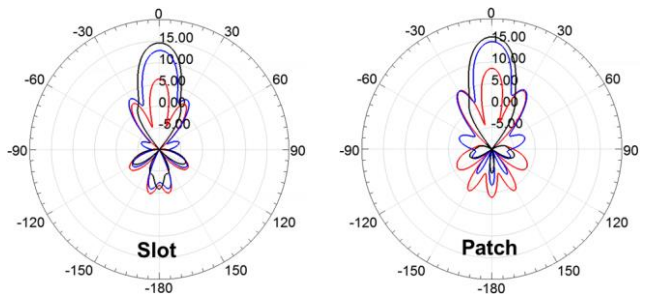

(b) H-plane

Fig. 6. Simulated far-field radiation patterns at 11.2GHz: FPC antenna system with slot (left) or patch (right): FSS-AH (**black**), FSS-1V (**blue**), FSS-3V (**red**)

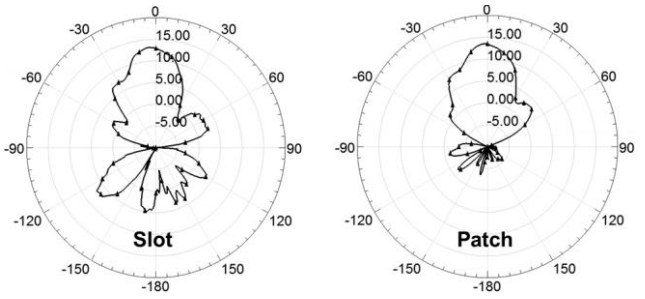

(a) E-plane

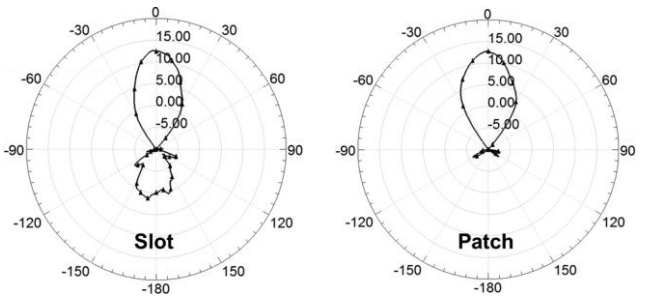

(b) H-plane

Fig. 7. Measured far-field radiation patterns for FSS-AH: FPC antenna system with slot at 10.81GHz (left) or patch at 10.85GHz (right)

The beamwidth for slot is reduced to 21˚ and for patch is maintained at 27˚. It demonstrates that the inclusion of one vertical column reduces the radiation leakage through the FSS in the center of the source. The result is reduced peak gain and increased back lobe for the slot, and reduced peak gain and increased side lobe for the patch. For FSS-3V design, the peak gain drops significantly and the slot has more back radiation. The patch has more side lobe. It implies that vertical slots block the energy from the source to make reflection inside the cavity higher thus leading to increase in energy leakage out of the cavity sides.

In the H-plane, the overall response is most similar between the FSS-AH and FSS-1V case, except the side lobe increase for the patch case. The FSS-3V case with higher reflective surfaces in the center of the FPC produces much lower far-field radiation and higher back radiation. This is due to the leakage out of the cavity sides. The measured far-field pattern for the FSS-AH design is shown in Fig. 7. The best radiation pattern in this case was obtained at 10.81GHz and 10.85GHz, respectively, for slot and patch.

IV. Conclusion

This study illustrates the impact that the FSS designs have on the performance of slot and patch in an FPC system. The vertical augmentations result in horizontal beam-splitting in the near-field. We also demonstrate that the location of the beam is controlled by the width of vertical columns and there appears to be an optimum distance to maintain linear separation in the same plane. The work presented has open cavity sidewalls, which we believe create higher than expected back radiation. Future work will be compared to enclosed cavity structures as well as cavity-backed slot antenna designs. The proposed design offers the potential to synthesize array behavior in a single element FPC system.

Acknowledgment

This work is supported by the National Science Foundation under Award #1202329.

References

[1] Tianxia Zhao, David R. Jackson, Jeffery T. Williams, and Arthur A. Oliner, “General formulas for 2-D leaky-wave antennas,” IEEE Trans. Antennas Propag., vol. 53, no. 11, pp. 3525–3533, November 2005

[2] R. Gardelli, M. Albani, and F. Capolino, "Array thinning by using antennas in a Fabry-Perot cavity for gain enhancement," IEEE Trans. Antennas Propag., vol. 54, no. 7, pp. 1979–1990, July 2006

[3] A. P. Feresidis and J. C. Vardaxoglou, “A broadband high-gain resonant cavity antenna with single feed,” Proc. European Con. on Antennas and Propag. (EuCAP), Nice, France, pp. 1–5, November 2006

[4] Paolo Burghignoli, Giampiero Lovat, Filippo Capolino, David R. Jackson, and Donald R. Wilton, “Highly polarized, directive radiation from a Fabry-Pérot cavity leaky-wave antenna based on a metal strip grating,” IEEE Trans. Antennas Propag., vol. 58, no. 12, pp. 3873–3883, December 2010

[5] Muhammad U. Afzal and Karu P. Esselle, “Improving phase uniformity in the aperture: a method to enhance radiation characteristics of Fabry-Perot resonator antennas,” Proc. IEEE Int. Symp. Antennas Propag.,Vancouver, Canada, pp. 39–40, July 2015

[6] Chanjoon Lee, Robert Sainati, Rhonda Franklin, and Ramesh Harjani, “Comparative analysis of frequency selective surface geometry effect in Fabry-Perot Cavity antenna design” Proc. IEEE Wireless Microwave Technology Con., Cocoa Beach, FL, USA, pp. 1–4, April 2015

[7] Chanjoon Lee, Robert Sainati, Rhonda Franklin and Ramesh Harjani, “Fluidic switching and tunig of Fabry-Perot antenna,” Proc. IEEE Int. Symp. Antennas Propag.,Vancouver, Canada, pp. 2211–2212, July 2015